

# Genome-scale activation screen identifies a lncRNA locus regulating a gene neighbourhood

Julia Joung<sup>1,2,3,4</sup>, Jesse M. Engreitz<sup>2</sup>, Silvana Konermann<sup>2,3,4,†</sup>, Omar O. Abudayyeh<sup>2,3,4,5</sup>, Vanessa K. Verdine<sup>2,3</sup>, Francois Aguet<sup>2</sup>, Jonathan S. Gootenberg<sup>2,3,4,6</sup>, Neville E. Sanjana<sup>2,3,4,†</sup>, Jason B. Wright<sup>2,3,4</sup>, Charles P. Fulco<sup>2,6</sup>, Yuen-Yi Tseng<sup>2</sup>, Charles H. Yoon<sup>7</sup>, Jesse S. Boehm<sup>2</sup>, Eric S. Lander<sup>2,6,8</sup> & Feng Zhang<sup>1,2,3,4</sup>

Mammalian genomes contain thousands of loci that transcribe long noncoding RNAs (lncRNAs)<sup>1,2</sup>, some of which are known to carry out critical roles in diverse cellular processes through a variety of mechanisms<sup>3–8</sup>. Although some lncRNA loci encode RNAs that act non-locally (in *trans*)<sup>5</sup>, there is emerging evidence that many lncRNA loci act locally (in *cis*) to regulate the expression of nearby genes—for example, through functions of the lncRNA promoter, transcription, or transcript itself<sup>3,6–8</sup>. Despite their potentially important roles, it remains challenging to identify functional lncRNA loci and distinguish among these and other mechanisms. Here, to address these challenges, we developed a genome-scale CRISPR–Cas9 activation screen that targets more than 10,000 lncRNA transcriptional start sites to identify noncoding loci that influence a phenotype of interest. We found 11 lncRNA loci that, upon recruitment of an activator, mediate resistance to BRAF inhibitors in human melanoma cells. Most candidate loci appear to regulate nearby genes. Detailed analysis of one candidate, termed *EMICERI*, revealed that its transcriptional activation resulted in dosage-dependent activation of four neighbouring protein-coding

genes, one of which confers the resistance phenotype. Our screening and characterization approach provides a CRISPR toolkit with which to systematically discover the functions of noncoding loci and elucidate their diverse roles in gene regulation and cellular function.

We have previously used the Cas9 synergistic activation mediator (SAM) to screen for protein-coding genes that confer resistance to the BRAF inhibitor vemurafenib in melanoma cells<sup>9</sup>, making this an ideal phenotype for screening lncRNA loci (Supplementary Note 1). We designed a genome-scale single guide RNA (sgRNA) library that targeted 10,504 intergenic lncRNA transcriptional start sites (TSSs)<sup>2,10</sup> (see Methods, Supplementary Table 1). We transduced A375 (BRAF(V600E)) human melanoma cells with the sgRNA library, cultured them in 2  $\mu$ M vemurafenib or vehicle control for 14 days, and sequenced the distribution of sgRNAs (Fig. 1a, b and Extended Data Fig. 1a). RNAi gene enrichment ranking (RIGER) analysis<sup>11</sup> identified 16 candidate loci that were significantly enriched (FDR < 0.05) in cells cultured with vemurafenib (Extended Data Fig. 1b–e and Supplementary Table 2), none of which had previously been functionally characterized.

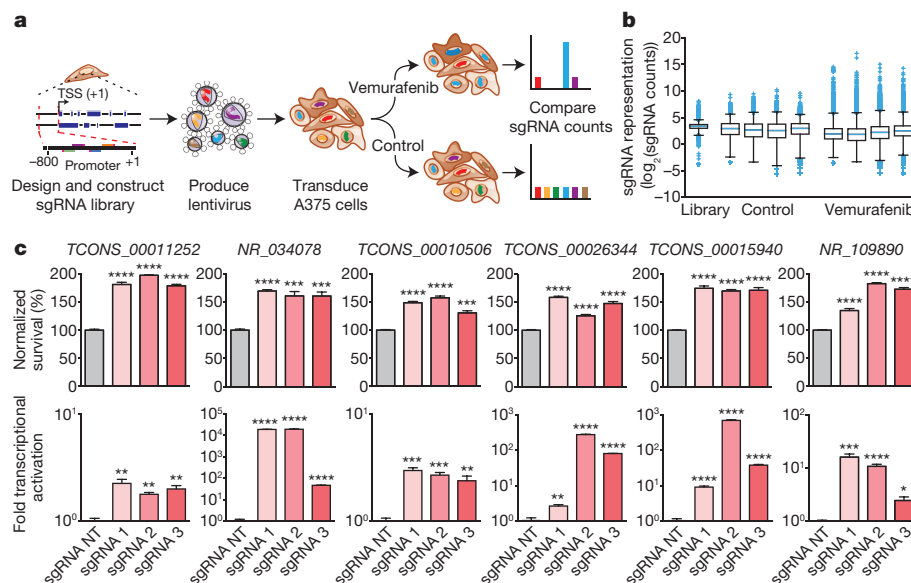


**Figure 1 | Genome-scale activation screen identifies lncRNA loci involved in vemurafenib resistance.** **a**, A375 cells expressing SAM effectors were transduced with the pooled sgRNA library targeting more than 10,000 lncRNA TSSs and treated with vemurafenib or control for 14 days before deep sequencing. **b**, Box plot showing sgRNA frequencies

after vemurafenib or control treatment from  $n = 4$  infection replicates. **c**, Vemurafenib resistance and transcriptional activation in A375 cells upon SAM activation of candidate lncRNA loci. NT, non-targeting. All values are mean  $\pm$  s.e.m. with  $n = 4$ . \*\*\*\* $P < 0.0001$ ; \*\*\* $P < 0.001$ ; \*\* $P < 0.01$ ; \* $P < 0.05$ .

<sup>1</sup>Department of Biological Engineering, MIT, Cambridge, Massachusetts 02139, USA. <sup>2</sup>Broad Institute of MIT and Harvard, Cambridge, Massachusetts 02142, USA. <sup>3</sup>McGovern Institute for Brain Research at MIT, Cambridge, Massachusetts 02139, USA. <sup>4</sup>Department of Brain and Cognitive Science, MIT, Cambridge, Massachusetts 02139, USA. <sup>5</sup>Division of Health Sciences and Technology, MIT, Cambridge, Massachusetts 02139, USA. <sup>6</sup>Department of Systems Biology, Harvard Medical School, Boston, Massachusetts 02115, USA. <sup>7</sup>Department of Surgery, Brigham and Women's Hospital, Boston, Massachusetts 02115, USA. <sup>8</sup>Department of Biology, MIT, Cambridge, Massachusetts 02139, USA. †Present addresses: Salk Institute for Biological Studies, La Jolla, California, USA (S.K.); New York Genome Center, New York, New York, USA (N.E.S.); Department of Biology, New York University, New York, New York, USA (N.E.S.).

To validate the screening results, we individually expressed the three most enriched sgRNAs targeting each of the top 16 candidate lncRNA loci in A375 cells. In all 16 cases, the sgRNAs conferred significant vemurafenib resistance ( $P < 0.01$ ) (Extended Data Fig. 2), verifying the robustness of our screening approach. We performed RNA sequencing upon activation of each of the 11 loci that showed the strongest effects (Extended Data Fig. 2, Supplementary Table 3) and found global changes in gene expression consistent with vemurafenib resistance, supporting the functional relevance of these loci to the screening phenotype (Extended Data Fig. 3a).

Next, we turned to classifying the mechanisms by which activation of each of these loci might lead to resistance. These mechanisms could include (i) a non-local (*trans*) function of the lncRNA transcript<sup>5</sup>, (ii) a local (*cis*) function of the lncRNA transcript or its transcription in affecting the expression of a nearby gene<sup>3,6–8</sup>, (iii) a local function of the lncRNA promoter acting as a DNA element (enhancer)<sup>7,8</sup>, and, in theory, (iv) a local function of SAM (Supplementary Note 2). To study the first two of these mechanisms, which require the lncRNA or its transcription, we focused on the 6 of 11 loci at which SAM targeting led to robust upregulation of the lncRNA transcript (Fig. 1c, Supplementary Table 3). The remaining five loci may function through a mechanism other than activation of the lncRNA transcript (for example, the third and fourth mechanisms above; Supplementary Note 3 and Supplementary Table 4).

We investigated whether activating each of these six lncRNA loci might affect vemurafenib resistance through non-local or local functions. To test whether candidate lncRNAs contributed to vemurafenib resistance via non-local functions, we overexpressed cDNAs encoding each lncRNA from randomly integrated lentivirus. We did not find any that affected drug resistance (Extended Data Fig. 3b), suggesting that these loci are not likely to act through non-local functions (Supplementary Note 4 and Supplementary Table 3). To determine whether the phenotype might result instead from local functions of the lncRNA loci in regulating a nearby gene<sup>3,6,7</sup>, we examined the expression of all genes within 1 Mb of the targeted sites. At five of the six loci, SAM targeting led to differential expression of between one and eight nearby protein-coding genes (Supplementary Table 4; for

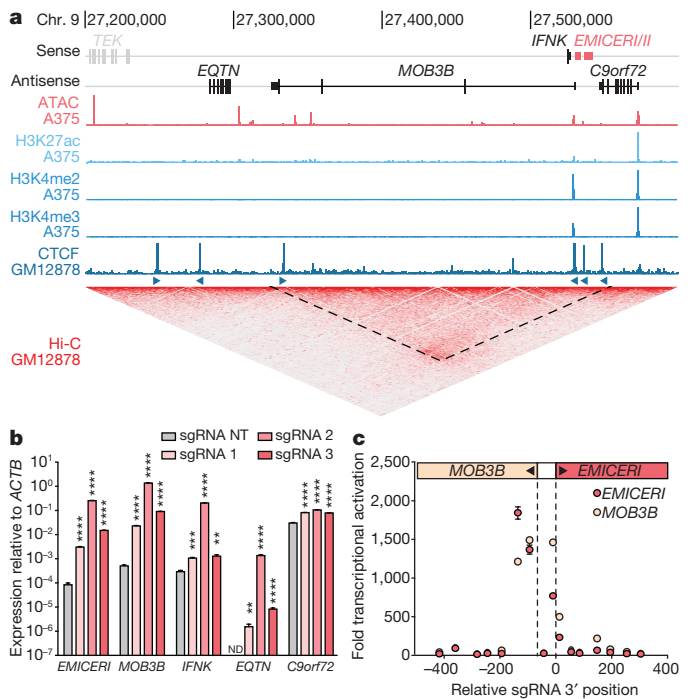


**Figure 2 | Activation of the *EMICERI* promoter results in dose-dependent upregulation of neighbouring genes.** **a**, Genomic locus of *EMICERI* contains four neighbouring genes (*EQTN*, *MOB3B*, *IFNK* and *C9orf72*) and a topological domain. **b**, Expression of *EMICERI* and its neighbouring genes after targeting SAM to the *EMICERI* promoter. **c**, Expression of *EMICERI* and *MOB3B* upon tiling SAM across the *EMICERI* locus normalized to a non-targeting sgRNA. All values are mean  $\pm$  s.e.m. with  $n = 4$ . \*\*\*\* $P < 0.0001$ ; \*\*\* $P < 0.001$ ; \*\* $P < 0.01$ . ND, not detected.

remaining locus, see Supplementary Note 5). For example, activation of *NR\_109890* upregulated its neighbouring gene *EBF1* (Extended Data Fig. 3c), and activation of *TCONS\_00015940* led to dosage-dependent

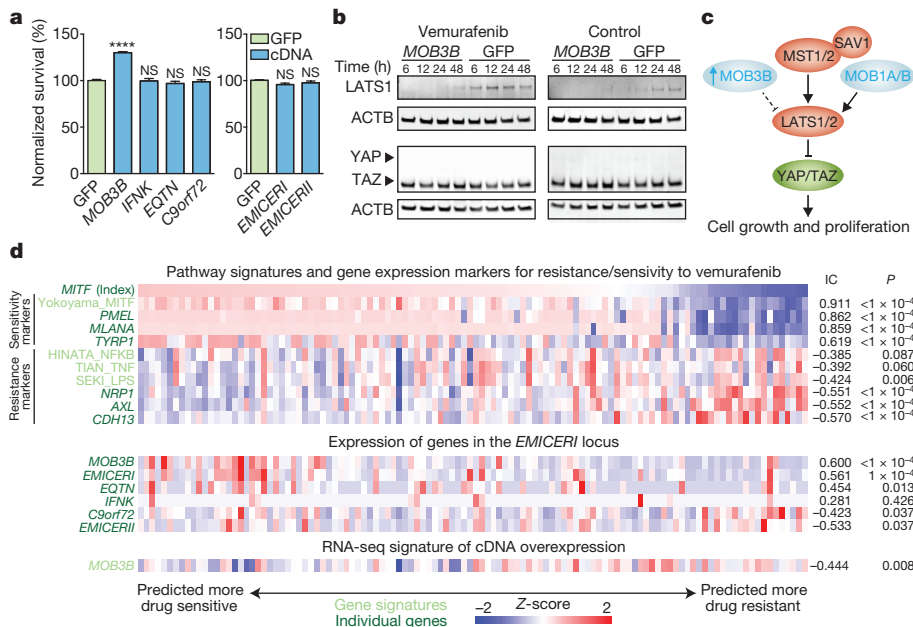


**Figure 3 | *MOB3B* mediates vemurafenib resistance through the Hippo signalling pathway.** **a**, Vemurafenib resistance of A375 cells overexpressing each neighbouring gene or lncRNA. All values are mean  $\pm$  s.e.m. with  $n = 4$ . \*\*\*\* $P < 0.0001$ . NS, not significant. **b**, Western blots of A375 cells overexpressing *MOB3B*. For gel source images, see Supplementary Fig. 1. **c**, Proposed mechanism of *MOB3B*. **d**, Expression

of gene or signature markers for BRAF inhibitor sensitivity (top), genes in the *EMICERI* locus (middle) and *MOB3B* overexpression RNA sequencing (RNA-seq) signature (bottom) in BRAF(V600) patient melanomas from The Cancer Genome Atlas (see Methods for signature generation). IC, information coefficient.

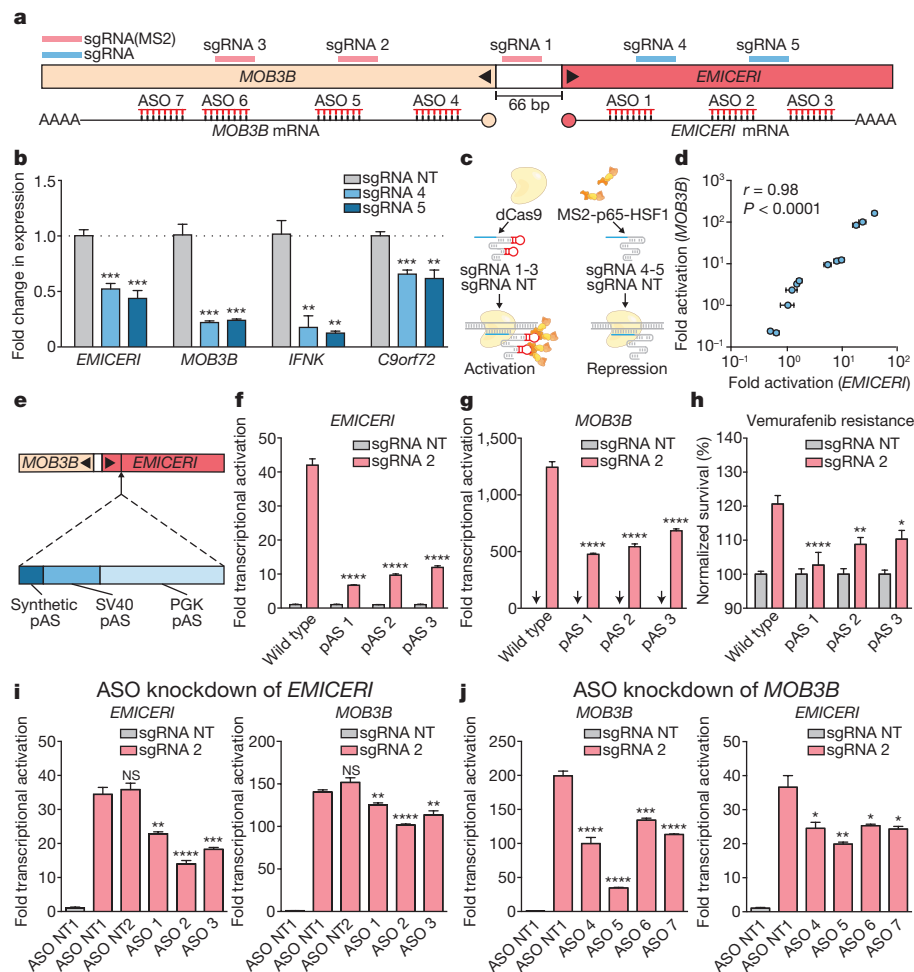


**Figure 4** | *EMICERI* transcription modulates *MOB3B* expression.

**a**, sgRNA and ASO positions. **b**, Expression of genes in the *EMICERI* locus upon dCas9 targeting. **c**, Bimodal perturbation schematic. **d**, *MOB3B* and *EMICERI* expression levels after bimodal perturbation. **e**, pAS insertion schematic. SV40, Simian virus 40; PGK, phosphoglycerate kinase.

**f–h**, *EMICERI* expression, *MOB3B* expression and vemurafenib resistance in pAS clones. **i**, **j**, *EMICERI* and *MOB3B* expression after ASO knockdown. Mean  $\pm$  s.e.m.,  $n = 4$ . \*\*\*\* $P < 0.0001$ ; \*\*\* $P < 0.001$ ; \*\* $P < 0.01$ ; \* $P < 0.05$ . NS, not significant.

upregulation of four neighbouring genes (Fig. 2a, b). Thus, most candidate lncRNA loci appear to confer vemurafenib resistance by regulating the expression of one or more nearby genes, including some that have been previously implicated in vemurafenib resistance (for example, *EBF1*; see Supplementary Table 3).

To further elucidate the mechanism for one of these candidate local regulators, we focused on *TCONS\_00015940*, which, when targeted, led to a dosage-dependent activation of the four closest nearby genes (*EQTN*, *MOB3B*, *IFNK*, and *C9orf72*) (Fig. 2a, b). The targeted site is a putative enhancer marked by assay for transposase-accessible chromatin (ATAC) and histone H3 lysine-27 acetylation (H3K27ac) that is proximal to the boundary of a topological domain (Fig. 2a and Extended Data Fig. 4). Upon examining this locus, we found that *TCONS\_00015940* comprises two separate transcripts (Extended Data Fig. 5a and Supplementary Note 6). We named these transcripts *EQTN MOB3B IFNK C9orf72* enhancer RNA I and II, or *EMICERI* and *EMICERII*. The *EMICERI* promoter, which we targeted in our screen, produces two divergent transcripts that initiate about 66 base pairs (bp) apart: *EMICERI* and *MOB3B*, a protein-coding gene (Fig. 2a). Tiling SAM across this region indicated that targeting an approximately 200-bp region activated both of these genes (Fig. 2a, c). By contrast, targeting SAM to the promoters of the other three nearby genes did not produce coordinated transcriptional activation in the region (Extended Data Fig. 5b and Supplementary Note 7). These results demonstrate that the *EMICERI*-*MOB3B* promoter influences gene expression in a roughly 300-kb gene neighbourhood.

To determine how coordinated upregulation of the *EMICERI* gene neighbourhood led to vemurafenib resistance, we overexpressed cDNAs encoding each of the four protein-coding genes and *EMICERI* or *EMICERII* lncRNAs from randomly integrated lentivirus. Overexpression of one of the six genes, *MOB3B*, was sufficient to induce the resistance phenotype (Fig. 3a, Extended Data Fig. 6 and Supplementary Note 8). Notably, *MOB3B* is a kinase activator that is a paralogue of *MOB1A* and *MOB1B*, known components of the Hippo signalling pathway, whose activation has been shown to confer vemurafenib resistance<sup>12,13</sup>. *MOB3B* overexpression downregulated large tumor suppressor kinase 1 (LATS1) to activate the Hippo signalling pathway (Fig. 3b, c, Extended Data Fig. 7a–c and Supplementary Note 9). Activation of *EMICERI* and *MOB3B* conferred vemurafenib resistance in two additional vemurafenib-sensitive melanoma cell lines besides the one used in our initial screen (Extended Data Fig. 7d–f), and the effects of activation on gene expression correlated with a signature of vemurafenib resistance in patient melanomas (Fig. 3d, Extended Data Figs 3, 8 and Supplementary Note 9). Together, these results indicate that activation of the *EMICERI* locus confers vemurafenib resistance through upregulation of *MOB3B* and subsequent activation of the Hippo signalling pathway.

We next investigated whether upregulation of the *EMICERI* transcript is required for full *MOB3B* activation, because targeting SAM to the shared *EMICERI*-*MOB3B* promoter (Fig. 4a) could directly activate *MOB3B* to confer resistance. Accordingly, we used three perturbation methods to interfere with *EMICERI* transcription and observed effects on *MOB3B*.

First, to block transcription of *EMICERI*, we targeted dCas9 downstream of the *EMICERI* TSS. This intervention reduced the expression of *EMICERI*, *MOB3B* and the other neighbouring genes (Fig. 4a, b). We then used a bimodal perturbation system that uses an sgRNA without the SAM-recruitment sequences to target dCas9 to block *EMICERI* transcription and an sgRNA with the SAM-recruitment sequences to activate the promoter region (Fig. 4a, c). Different combinations of repression and activation sgRNAs demonstrated that the transcriptional levels of *EMICERI* and *MOB3B* were tightly coupled across several orders of magnitude ( $r = 0.98$ ,  $P < 0.0001$ ; Fig. 4d).

Second, we generated clonal A375 cell lines carrying insertions of three tandem polyadenylation signals (pAS) downstream of the *EMICERI* TSS, which eliminated most of the *EMICERI* RNA without disrupting the promoter sequence (Fig. 4e, Extended Data Fig. 9a–c and Supplementary Note 10). Upon SAM activation, the pAS-insertion clones showed reduced expression of *EMICERI*, *MOB3B* and the three other nearby genes compared to wild-type clones (Fig. 4f, g and Extended Data Fig. 9d–f), and, as expected, reduced vemurafenib resistance (Fig. 4h and Extended Data Fig. 9g, h). This provides genetic evidence that transcription of *EMICERI* is involved in *MOB3B* activation.

Third, in the context of SAM activation, we knocked down the *EMICERI* transcript by transient transfection with antisense oligonucleotides (ASOs; Fig. 4a), which can lead to cleavage of nascent transcripts by RNase H and transcriptional termination (Supplementary Note 11). ASOs targeting *EMICERI* reduced the expression of both *EMICERI* and *MOB3B* in a dosage-dependent manner (Fig. 4i and Extended Data Fig. 10a), consistent with the dCas9 and pAS insertion results.

These *EMICERI* perturbation experiments demonstrate that transcription of *EMICERI* is required for full activation of *MOB3B*, confirming that *EMICERI* is a functional noncoding locus that activates four neighbouring protein-coding genes and contributes to the screening phenotype. The precise mechanism may involve either the *EMICERI* transcript or its transcription<sup>7,14</sup>.

To determine whether *MOB3B* transcription could reciprocally regulate *EMICERI* expression, we perturbed *MOB3B* transcription and observed the effects on *EMICERI*. We found that targeting dCas9 downstream of the *MOB3B* TSS successfully blocked *MOB3B* transcription and reduced expression of *EMICERI* and other neighbouring genes (Extended Data Fig. 10b); similarly, in the context of SAM activation, ASOs targeting *MOB3B* introns reduced the activation of both *MOB3B* and *EMICERI* (Fig. 4j and Extended Data Fig. 10c). Together, the *EMICERI* and *MOB3B* perturbation experiments suggested that transcription of both the lncRNA and the mRNA regulate one another in a positive feedback mechanism that then activates a broader gene neighbourhood, potentially through general processes associated with transcription<sup>7,14</sup>.

An important challenge in understanding the regulatory logic of the genome has been to identify functional lncRNA loci and characterize their mechanisms. Here we demonstrate that genome-scale activation screens enable systematic identification of lncRNA loci that influence a specific cellular process. We provide a framework for distinguishing categories of lncRNA mechanisms, including non-local functions as well as a diverse array of possible local regulatory mechanisms. Notably, the candidate lncRNA loci we identified appear to act locally to regulate nearby gene expression, including a remarkable case involving coordinated activation of four nearby genes. Further application of our noncoding gain-of-function screening approach, together with loss-of-function screening methods<sup>15–18</sup> and our characterization strategy, will help to elucidate the complex roles of the noncoding genome in development and disease.

**Online Content** Methods, along with any additional Extended Data display items and Source Data, are available in the online version of the paper; references unique to these sections appear only in the online paper.

Received 24 January; accepted 30 June 2017.

Published online 11 August 2017.

- Guttman, M. *et al.* Chromatin signature reveals over a thousand highly conserved large non-coding RNAs in mammals. *Nature* **458**, 223–227 (2009).
- Cabili, M. N. *et al.* Integrative annotation of human large intergenic noncoding RNAs reveals global properties and specific subclasses. *Genes Dev.* **25**, 1915–1927 (2011).
- Wang, K. C. *et al.* A long noncoding RNA maintains active chromatin to coordinate homeotic gene expression. *Nature* **472**, 120–124 (2011).
- Engreitz, J. M. *et al.* The Xist lncRNA exploits three-dimensional genome architecture to spread across the X chromosome. *Science* **341**, 1237973 (2013).
- Kretz, M. *et al.* Control of somatic tissue differentiation by the long non-coding RNA TINCR. *Nature* **493**, 231–235 (2013).
- Anderson, K. M. *et al.* Transcription of the non-coding RNA upperhand controls Hand2 expression and heart development. *Nature* **539**, 433–436 (2016).
- Engreitz, J. M. *et al.* Local regulation of gene expression by lncRNA promoters, transcription and splicing. *Nature* **539**, 452–455 (2016).
- Paralkar, V. R. *et al.* Unlinking an lncRNA from its associated *cis* element. *Mol. Cell* **62**, 104–110 (2016).
- Konermann, S. *et al.* Genome-scale transcriptional activation by an engineered CRISPR–Cas9 complex. *Nature* **517**, 583–588 (2015).
- O’Leary, N. A. *et al.* Reference sequence (RefSeq) database at NCBI: current status, taxonomic expansion, and functional annotation. *Nucleic Acids Res.* **44**, D733–D745 (2016).
- König, R. *et al.* A probability-based approach for the analysis of large-scale RNAi screens. *Nat. Methods* **4**, 847–849 (2007).
- Johannessen, C. M. *et al.* A melanocyte lineage program confers resistance to MAP kinase pathway inhibition. *Nature* **504**, 138–142 (2013). 10.1038/nature12688
- Praskova, M., Xia, F. & Avruch, J. MOBKL1A/MOBKL1B phosphorylation by MST1 and MST2 inhibits cell proliferation. *Curr. Biol.* **18**, 311–321 (2008).
- Skalska, L., Beltran-Nebot, M., Ule, J. & Jenner, R. G. Regulatory feedback from nascent RNA to chromatin and transcription. *Nat. Rev. Mol. Cell Biol.* **18**, 331–337 (2017).
- Fulco, C. P. *et al.* Systematic mapping of functional enhancer–promoter connections with CRISPR interference. *Science* **354**, 769–773 (2016).
- Liu, S. J. *et al.* CRISPRi-based genome-scale identification of functional long noncoding RNA loci in human cells. *Science* **355**, aah7111 (2017).
- Sanjana, N. E. *et al.* High-resolution interrogation of functional elements in the noncoding genome. *Science* **353**, 1545–1549 (2016).
- Zhu, S. *et al.* Genome-scale deletion screening of human long non-coding RNAs using a paired-guide RNA CRISPR–Cas9 library. *Nat. Biotechnol.* **34**, 1279–1286 (2016).

**Supplementary Information** is available in the online version of the paper.

**Acknowledgements** We thank M. Guttman, C. M. Johannessen and M. Ghandi for helpful discussions and insights; A. Sayeed, R. Deasy, A. Rotem and B. Izar for generating the primary patient melanoma cell lines; and R. Belliveau, R. Macrae and the Zhang laboratory for support and advice. J.M.E. is supported by the Fannie and John Hertz Foundation. O.A.A. is supported by a Paul and Daisy Soros Fellowship and National Defense Science and Engineering Fellowship. J.S.G. is supported by a DOE Computational Science Graduate Fellowship. N.E.S. is supported by the NIH through NHGRI (R00-HG008171). J.B.W. is supported by the NIH through NIDDK (F32-DK096822). C.P.F. is supported by the National Defense Science and Engineering Graduate Fellowship. E.S.L. is supported by UM1HG008895 and funds from the Broad Institute. F.Z. is a New York Stem Cell Foundation–Robertson Investigator. F.Z. is supported by the NIH through NIMH (5DP1-MH100706 and 1R01-MH110049), NSF, Howard Hughes Medical Institute, the New York Stem Cell, Simons, Paul G. Allen Family, and Vallee Foundations; and James and Patricia Poitras, Robert Metcalfe, and David Cheng.

**Author Contributions** J.J., S.K. and F.Z. conceived and designed the study. J.J. and S.K. conducted the screen. J.J., V.K.V. and J.S.G. performed validation experiments. N.E.S. and J.B.W. performed ATAC–seq and ChIP experiments. J.J. analysed data. O.O.A. and F.A. analysed clinical datasets. J.M.E., C.P.F. and E.S.L. helped with lncRNA experimental design and interpretation. Y.-Y.T., C.H.Y. and J.S.B. generated primary patient melanoma cell lines. J.J., J.M.E., E.S.L. and F.Z. wrote the paper with help from all authors.

**Author Information** Reprints and permissions information is available at [www.nature.com/reprints](http://www.nature.com/reprints). The authors declare competing financial interests: details are available in the online version of the paper. Readers are welcome to comment on the online version of the paper. Publisher’s note: Springer Nature remains neutral with regard to jurisdictional claims in published maps and institutional affiliations. Correspondence and requests for materials should be addressed to F.Z. ([zhang@broadinstitute.org](mailto:zhang@broadinstitute.org)) or E.S.L. ([lander@broadinstitute.org](mailto:lander@broadinstitute.org)).

## METHODS

**Design and cloning of SAM lncRNA library.** RefSeq noncoding RNAs (release 69) were filtered for lncRNA transcripts that were longer than 200 bp and did not overlap with RefSeq coding gene isoforms<sup>10</sup>. The RefSeq lncRNA catalogue was combined with the Cabili lncRNA catalogue and filtered for unique lncRNA TSSs, defined as TSSs that were >50 bp apart<sup>2</sup>. This resulted in 10,504 unique lncRNA TSSs that were targeted with ~10 sgRNAs each for a total library of 95,958 sgRNAs. sgRNAs were designed to target the first 800 bp upstream of each TSS and subsequently filtered for GC content >25%, minimal overlap of the target sequence, and homopolymer stretch <4 bp. After filtering, the remaining sgRNAs were scored according to predicted off-target matches as described previously<sup>9</sup>, and six sgRNAs with the best off-target scores were selected in the first 200-bp region upstream of the TSS: one in the 200–300-bp region, one in the 300–400-bp region, one in the 400–600-bp region, and one in the 600–800-bp region. In regions with an insufficient number of possible sgRNAs, sgRNAs were selected from the neighbouring region closer to the TSS. The ideal location for sgRNA targeting to achieve maximal activation, either upstream or downstream of the TSS, may be unique for each lncRNA locus and dependent on the local regulatory context (for example, locations of TF binding sites). An additional 500 non-targeting sgRNAs were included as controls. Cloning of the SAM sgRNA libraries was performed as previously described with a minimum representation of 100 transformed colonies per sgRNA followed by next-generation sequencing (NGS) validation<sup>19</sup>.

**Lentivirus production and transduction.** For transduction, plasmids were packaged into lentivirus through transfection of library plasmid with appropriate packaging plasmids (psPAX2: Addgene 12260; pMD2.G: Addgene 12259) using Lipofectamine 2000 (Thermo Fisher 11668019) and Plus reagent (Thermo Fisher 11514015) in HEK293FT (Thermo Fisher R70007) as described previously<sup>19</sup>. The HEK293FT cell line is on the list of commonly misidentified cell lines maintained by the International Cell Line Authentication Committee, and has not been authenticated or tested for mycoplasma contamination. HEK293FT cells are most commonly used for lentivirus production because they are easy to transfect and produce lentivirus very efficiently. Human melanoma A375 cells (Sigma-Aldrich 88113005) were cultured in R10 medium: RPMI 1640 (Thermo Fisher 61870) supplemented with 10% FBS (VWR 97068-085) and 1% penicillin/streptomycin (Thermo Fisher 15140122). A375 cells have not been tested for mycoplasma contamination. Cells were passaged every other day at a 1:5 ratio. Concentrations for selection agents were determined using a kill curve: 300 µg/ml zeocin (Thermo Fisher R25001), 10 µg/ml blasticidin (Thermo Fisher A1113903), and 300 µg/ml hygromycin (Thermo Fisher 10687010). Cells were transduced by spinfection and selected with the appropriate antibiotic as described previously<sup>19</sup>. During selection, medium was refreshed when cells were passaged every 3 days. The duration of selection was 7 days for zeocin and 5 days for hygromycin and blasticidin. Lentiviral titres were calculated by spinfecting cells with five different volumes of lentivirus and determining viability after a complete selection of 3 days<sup>19</sup>.

**Vemurafenib resistance screen.** The vemurafenib resistance screen was conducted similarly to a previously described genome-scale SAM coding gene screen<sup>9</sup>. A375 cells stably integrated with dCas9-VP64 (Addgene 61425) and MS2-P65-HSF1 (Addgene 61426) were transduced with the pooled sgRNA library (Addgene 61427) as described above at an MOI of 0.3 for a total of four infection replicates, with a minimal representation of 500 transduced cells per sgRNA in each replicate. Cells were maintained at >500 cells per sgRNA during subsequent passaging. After 7 days of zeocin selection and 2 days of no antibiotic selection, cells were split into control (DMSO) and vemurafenib (2 µM PLX-4720 dissolved in DMSO, Selleckchem S1152) conditions. Cells were passaged every 2 days for a total of 14 days of control or vemurafenib treatment. The 14-day screening duration was selected based on previous studies<sup>9,17</sup>. At the end of the screening selection, >500 cells per sgRNA in each condition were harvested for gDNA extraction and amplification of the virally integrated sgRNAs as described previously<sup>19</sup>. Resulting libraries were deep-sequenced on Illumina MiSeq or NextSeq platforms with a coverage of >25 million reads passing filter per library.

**NGS and screen hits analysis.** NGS data were de-multiplexed using unique index reads. sgRNA counts were determined on the basis of perfectly matched sequencing reads only. For each condition, a pseudocount of 1 was added to the sgRNA count and the counts were normalized to the total number of counts in the condition. The sgRNA fold change as a result of screening selection was calculated by dividing the normalized sgRNA counts in the vemurafenib condition by the control and taking the base-2 logarithm. RIGER<sup>11</sup> analysis was performed using GENE-E based on the normalized log<sub>2</sub> ratios for each infection replicate. As a low percentage of functional sgRNAs was expected for each lncRNA loci, the weighted sum method was used. To determine the empirical false discovery rate (FDR) of candidate lncRNA loci, the weighted sum for 10 randomly selected non-targeting sgRNAs in the sgRNA library was used to estimate the *P* value for each lncRNA locus and a threshold based on a FDR of 0.05 (Benjamini–Hochberg) was selected

that corresponded to a *P* value of 0.031. Seven candidate lncRNA loci were selected on the basis of average ranking between infection replicates 1 and 2, and nine candidate lncRNA loci were selected on the basis of average ranking in all four infection replicates. All candidate lncRNA loci had *P* < 10<sup>-5</sup>.

**Vemurafenib resistance assay.** A375 cells stably integrated with dCas9-VP64 and MS2-P65-HSF1 were transduced with individual sgRNAs targeting the 16 top candidate lncRNA loci from the vemurafenib resistance screen (3 sgRNAs with the highest enrichment per lncRNA locus; Supplementary Table 5) or with control non-targeting sgRNA at an MOI of <0.5 and selected with zeocin for 5 days as described above. For cDNA overexpression, A375 cells were transduced with cDNA (Supplementary Table 6) or control GFP at an MOI of <0.5 and selected with hygromycin for 4 days. To demonstrate that the results involving *EMICERI* and *MOB3B* extend to additional melanoma cell lines, A375 cells or additional melanoma cell lines (A2058, ATCC CRL-11147; COLO679, Sigma-Aldrich 87061210; UACC62, AddexBio C0020003) cultured in R10 medium were transduced with SAM effectors and *EMICERI*-targeting sgRNA 2 (Supplementary Table 7) or with control non-targeting sgRNA. Five days after transduction, cells were replated at low density (3 × 10<sup>3</sup> cells per well in a 96-well plate; four biological replicates per condition). Vemurafenib (2 µM) or control DMSO was added 3 h after plating and refreshed every 2 days for 3–4 days before cell viability was measured using CellTiter-Glo Luminescent Cell Viability Assay (Promega G7571). Significance testing was performed using two-sided Student's *t*-test. For primary patient tumour-derived melanoma cell lines, cells were plated at low density (2 × 10<sup>3</sup> cells per well in a 96-well plate; four biological replicates per condition) and vemurafenib was added 24 h after plating. Cells were treated for 3 days before cell viability was measured. For vemurafenib dose–response curves, the indicated concentrations of vemurafenib were added and the normalized per cent survival values were fitted with a nonlinear curve (log[inhibitor] vs normalized response; Prism 6). Significant differences in logIC<sub>50</sub> values were determined using the extra sum-of-squares *F* test.

**qPCR quantification of transcript expression.** A375 cells or additional melanoma cell lines stably integrated with SAM components were transduced with individual sgRNAs targeting the top candidate lncRNA loci (Supplementary Table 5), perturbing the *EMICERI* locus (Supplementary Table 7), or non-targeting control at an MOI of <0.5 and selected with zeocin for 5 days as described above. For cDNA overexpression, A375 cells were transduced with cDNA (Supplementary Table 6) or control GFP at an MOI of <0.5 and selected with hygromycin for 4 days. Cells were plated 5 days after transduction at 70% confluency (3 × 10<sup>4</sup> cells per well in a 96-well plate; four biological replicates per condition, each with four technical replicates), and harvested for RNA 24 h after plating as described previously<sup>19</sup>. For transcripts that this method could not detect, cells transduced with the respective sgRNAs were plated 5 days after transduction (1.8 × 10<sup>5</sup> cells per well in a 24-well plate; three biological replicates per condition). RNA was harvested using the RNeasy Plus Mini Kit (Qiagen 74134) and 1 µg RNA was used for reverse transcription with the qScript Flex cDNA Kit (VWR 95049) and lncRNA-specific primers (Supplementary Table 8). After reverse transcription, TaqMan qPCR was performed with custom or readymade probes as described previously<sup>19</sup> (Supplementary Tables 6, 8). Significance testing was performed using a two-sided Student's *t*-test.

**RNA sequencing and data analysis.** A375 cells transduced with individual sgRNAs targeting candidate lncRNA loci or with control non-targeting sgRNAs (Supplementary Table 5) were plated 5 days after transduction at 9 × 10<sup>4</sup> cells per well or 1.8 × 10<sup>5</sup> cells per well, respectively, in a 24-well plate. Three biological replicates per condition were plated. For cDNA overexpression, A375 cells were transduced with cDNA (Supplementary Table 6) or control GFP at an MOI of <0.5 and selected with hygromycin for 4 days. Cells were treated with 2 µM vemurafenib for 3 days before RNA was harvested as described above. The six candidate lncRNA loci with detectable transcript upregulation were prepped with TruSeq Stranded Total RNA Sample Prep Kit with Ribo-Zero Gold (Illumina RS-122-2302) and all other samples were prepped with NEBNext Ultra RNA Library Prep Kit for Illumina (NEB E7530S) and NEBNext PAS mRNA Magnetic Isolation Module (NEB E7490S). Libraries were deep-sequenced on the Illumina NextSeq platform (>9 million reads per condition). A Bowtie<sup>20</sup> index was created, based on the human hg19 UCSC genome, and known gene and lncRNA transcriptomes were constructed as described above. Paired-end reads were aligned directly to this index using Bowtie<sup>20</sup> with command line options '-q-phred33-quals -n 2 -e 99999999 -l 25 -I 1 -X 1000 -chunkmbs 512 -p 1 -a -m 200 -S'. Next, RSEM v1.2.22<sup>21</sup> was run with default parameters on the alignments created by Bowtie to estimate expression levels.

RSEM's TPM estimates for each transcript were transformed to log-space by taking log<sub>2</sub>(TPM+1). Transcripts were considered detected if their transformed expression level was equal to or above 1 (in log<sub>2</sub>(TPM+1) scale). All genes detected in at least one library (out of three libraries per condition) were used to find

differentially expressed genes. For activation of lncRNA loci, the two-sided Student's *t*-test was performed on each of the three replicates for each targeting sgRNA against both non-targeting sgRNAs. For *MOB3B* cDNA overexpression, the *t*-test was performed on the cDNA overexpression against GFP control. Only genes that were significant (*P* value pass 0.05 FDR correction) were reported. For lncRNA loci activation, the genes overlapping all three targeting sgRNAs were reported as differentially expressed as a result of lncRNA loci activation. Power analysis for two-sided *t*-tests were performed on each targeting sgRNA against both non-targeting sgRNAs to determine the probability of correctly identifying a gene as differentially expressed.

For annotating *EMICERI*, TopHat<sup>22</sup> was used to align RNA-seq reads from A375 transduced with sgRNA 2 or sgRNA 3 (Supplementary Table 7) with command line options '-solexa-quals-num-threads 8-library-type fr-firststrand-transcriptome-max-hits 1-prefilter-multihits-keep-fasta-order'. To further investigate the mechanism for *MOB3B* overexpression, Ingenuity Pathway Analysis was applied to all genes that were differentially expressed with at least 1.2-fold change or less than 0.7-fold change and the most likely upstream regulator was reported.

**Hi-C and chromatin immunoprecipitation with sequencing (ChIP-seq) in GM12878.** *In situ* Hi-C data for GM12878 were obtained and visualized using a 2.5-kb-resolution KL-normalized observed matrix<sup>23</sup>. Hi-C data from seven cell lines suggested similar topological domain annotations as GM12878<sup>23</sup>, suggesting that the TAD present in GM12878 is consistent across cell types. CTCF ChIP-seq for GM12878 and hg19 generated by the ENCODE Project Consortium<sup>24</sup> was downloaded from the UCSC Genome Browser. CTCF motifs were identified using FIMO to search for the 'V\_CTCF\_01' and 'V\_CTCF\_02' position weight matrices from TRANSFAC as described previously<sup>15</sup>.

**Assay for transposable and accessible chromatin sequencing (ATAC-seq).** ATAC-seq samples were prepared as described previously<sup>17</sup>. The library was sequenced using the Illumina NextSeq platform at ~136 million paired-end reads. Samples were aligned to the human hg19 UCSC genome using Bowtie<sup>20</sup> with command line options '-chunkmbs 256 -p 24 -S -m 1 -X 2000'. For quality control, the duplicate read rate was measured using Picard-Tools Mark Duplicates (10–30%) and the mitochondrial read rate was measured by Bowtie alignment to chrM (<5%).

**PhastCons sequence conservation.** PhastCons data for primates (*n* = 10 animals), placental mammals (*n* = 33) and vertebrates (*n* = 46) for hg19 were downloaded from the UCSC Genome Browser and aligned to the *EMICERI* locus<sup>25</sup>.

**ChIP-seq for histone modifications.** ChIP samples were prepared as described previously<sup>17</sup>. In brief, A375 cells were plated in T-225 flasks and grown to 70–90% confluence. Formaldehyde was added directly to the growth medium for a final concentration of 1% for 10 min at 37 °C to initiate chromatin fixation. The entire two-day ChIP procedure was performed using the EZ-Magna ChIP HiSens Chromatin Immunoprecipitation Kit (Millipore 1710460) according to the manufacturer's protocol. Samples were pulse-sonicated with two rounds of 10 min (30 s on-off cycles, high frequency) in a rotating water bath sonicator (Diagenode Bioruptor) with 5 min on ice between each round. To detect histone modifications, antibodies (H3K4me2: Millipore 17-677, H3K4me3: Millipore 04-745, H3K27ac: Millipore 17-683) were optimized individually for each antibody to be 0.5 µl for one million cells. One microlitre of IgG (Millipore 12-370) was used for negative control.

After verifying that the IgG ChIP had minimal background, ChIP samples were prepped with NEBNext Ultra II DNA Library Prep Kit for Illumina (NEB E7645S) and deep-sequenced on the Illumina NextSeq platform (>60 million reads per condition). Bowtie<sup>20</sup> was used to align paired-end reads to the human hg19 UCSC genome with command line options '-q -X 500-sam-chunkmbs 512'. Next, Model-based analysis of ChIP-seq (MACS) was run with command line options '-g hs -B -S-call-subpeaks' to identify histone modifications.

**Western blot.** A375 cells transduced with *MOB3B* cDNA or GFP control were plated 5 days after transduction at  $1.8 \times 10^5$  cells per well in a 24-well plate. Cells were treated with 2 µM vemurafenib for 6, 12, 24 or 48 h before protein lysates were harvested with RIPA lysis buffer (Cell Signaling Technologies 9806S) containing protease inhibitor (Roche 05892791001) and phosphatase inhibitor (Cell Signaling Technologies 5870S) cocktails. Samples standardized for protein concentration with the Pierce BCA protein assay (Thermo Fisher 23227) were incubated at 70 °C for 10 min under reducing conditions. After denaturation, 10 µg of the samples were separated using Bolt 4–12% Bis-Tris Plus Gels (Thermo Fisher NW04120BOX) and transferred onto a polyvinylidene difluoride membrane using iBlot Transfer Stacks (Thermo Fisher IB401001). Blots were blocked with Odyssey Blocking Buffer (TBS; LiCoR 927-50000) and probed with different primary antibodies (anti-pERK (Cell Signaling Technologies 4370, 1:2,000 dilution), anti-ERK (Cell Signaling Technologies 4695, 1:1,000 dilution), anti-pAKT (Ser473, Cell Signaling Technologies 4060, 1:1,000 dilution), anti-AKT (Cell Signaling Technologies 4691, 1:1,000 dilution), anti-LATS1 (Cell Signaling

Technologies 3477, 1:1,000 dilution), anti-YAP/TAZ (Cell Signaling Technologies 8418, 1:1,000 dilution), anti-MST1 (Cell Signaling Technologies 3682, 1:1,000 dilution) and anti-ACTB (Sigma A5441, 1:5,000 dilution)) overnight at 4 °C. Blots were then incubated with secondary antibodies IRDye 680RD Donkey anti-Mouse IgG (LiCoR 925-68072) and IRDye 800CW Donkey anti-Rabbit IgG (LiCoR 925-32213) at 1:20,000 dilution in Odyssey Blocking Buffer for 1 h at room temperature. p-ERK and p-AKT blots were stripped with Restore PLUS Western Blot Stripping Buffer (Thermo Fisher 46430) before probing for ERK and AKT, respectively. Blots were imaged using the Odyssey CLx (LiCoR).

**Primary patient melanoma-derived cell lines.** CLF\_SKCM\_001\_T and CLF\_SKCM\_004\_T melanoma tumour tissues were obtained from the Dana-Farber Cancer Institute hospital with informed consent and the cancer cell model line generation was approved by the ethical committee. Tumour tissues were dissected into tiny pieces using scalpels around 100 times. Dissected tissues were dissociated in collagenase-hyaluronidase (STEMCELL technologies 07912) medium for 1 h. Red blood cells were further depleted by adding ammonium chloride solution (STEMCELL technologies 07800). The dissociated cells were plated with smooth muscle growing medium-2 (Lonza CC-3181) in a six-well plate and split when the well confluency reached 80%. Cells were passaged five times with 1:4 splitting ratio for sequencing verification. The confirmed BRAF V600E melanoma cell models were propagated for another 7–15 passages and preserved in a cryovial. We used passage 12 cells for this study. All cells were fed every 3–4 days.

**Gene expression and pharmacological validation analysis.** Gene expression data (CCLE, TCGA) and pharmacological data (CCLE) were analysed to better understand the biological relevance of *EMICERI* and *MOB3B*. Transcript expression in TCGA and CCLE samples was quantified as follows: 1) FASTQ files were generated from available BAM files using SamToFastq in Picard Tools (<https://broadinstitute.github.io/picard/>); 2) reads were aligned with STAR v2.5.2b using parameters from the GTEx consortium pipeline (<https://github.com/broadinstitute/gtex-pipeline>) and genome indexes were generated for read lengths of 48 bp (TCGA) and 101 bp (CCLE) (-sjdbOverhang option); 3) expression was quantified using RSEM v1.2.22<sup>21</sup>. For the alignment and quantification steps, annotations for *TCONS\_00011252*, *NR\_034078*, *TCONS\_00010506*, *TCONS\_00026344*, *TCONS\_00015940\_1*, *TCONS\_00015940\_2*, and *NR\_109890* were appended to GENCODE 19 GTF (<https://www.encodegenes.org/releases/19.html>).

Gene expression (RNA-sequencing) data were collected from 113 BRAF<sup>V600</sup>-mutant primary and metastatic patient tumours from The Cancer Genome Atlas (TCGA: <https://portal.gdc.cancer.gov/>). Because pharmacological data were not available for the TCGA melanoma samples, signature gene sets were used to fully map the transcriptional BRAF-inhibitor-resistant or -sensitive states in TCGA as previously described<sup>26</sup>. The TCGA data set was used to determine the association between resistance and the expression of candidate lncRNA loci or genes in the *EMICERI* locus. In addition, we sought a more robust scoring system independent of any single gene. Gene expression signatures were generated based on the genes that were differentially expressed (top 1,000 most differentially expressed) as a result of candidate lncRNA loci or *MOB3B* overexpression identified from RNA-seq. Using single-sample Gene Set Enrichment Analysis (ssGSEA)<sup>27</sup>, a score was generated for each sample that represents the enrichment of the gene expression signature in that sample and the extent to which those genes are coordinately up- or downregulated. Patient tumours were also sorted by *EMICERI* expression to determine the correlation between expression of *EMICERI* and its neighbouring genes.

In the CCLE data set<sup>28</sup>, gene expression data (RNA-sequencing, CGHub: <https://portal.gdc.cancer.gov/>) and pharmacological data (activity area for MAPK pathway inhibitors) from BRAF<sup>V600</sup> mutant melanoma cell lines were used to compute the association between PLX-4720 resistance and the expression of genes in the *EMICERI* locus. Similar to the TCGA analysis, the *MOB3B* overexpression gene signature was determined using ssGSEA<sup>27</sup> projected onto the CCLE RNA-sequencing data set. Cell lines were also sorted by *EMICERI* expression to determine correlation between expression of *EMICERI* and its neighbouring genes.

To measure correlations between different features (signature scores, gene expression, or drug-resistance data) in the external cancer data sets, an information-theoretic approach (information coefficient; IC) was used and significance was measured using a permutation test (*n* = 10,000), as previously described<sup>26</sup>. The IC was calculated between the feature used to sort the samples (columns) in each data set and each of the features plotted in the heat map (pharmacological data, gene expression, and signature scores).

**pAS insertion.** To truncate *EMICERI*, the following pAS sequences were inserted in tandem 103, 156, and 198 bp downstream of each copy of the *EMICERI* TSS: Synthetic pAS: AATAAAAGATCTTTATTTTCATTAGATCTGTGTGTGGTGGTTTTTGTGTG SV40 pAS: GTTTATTGACGCTTATAATGGTTACAAATAAAGCAATAGCA TCACAAATTTACAAATAAAGCATTTTTTCTACTGCATTCTAGTTGTGG TTTGTCCAAACTCATCAATGTATCTTATCATGTCT

PGK pAS: AAATTGATGATCTATTAACAATAAAGATGTCCACTAAAAT  
GGAAGTTTTTCCTGTCATACTTTGTTAAGAAGGGTGAGAACAGAGTAC  
CTACATTTTGAATGGAAGGATTGGAGCTACGGGGGTGGGGTGGGGT  
GGATTAGATAAATGCCTGCTCTTACTGAAGGCTCTTACTATTGCTTT  
ATGATAATGTTTCATAGTTGGATATCATAATTTAAACAAGCAAACCAA  
TTAAGGGCCAGCTCATTCTCCACTCACGATCTATA

pAS clones were generated using CRISPR–Cas9-mediated homology-directed repair (HDR). Three sgRNAs targeting 103, 156 and 198 bp downstream of the *EMICERI* TSS (HDR sgRNA 1–3, Supplementary Table 9) and corresponding pAS HDR plasmids were used to insert pAS into each of the three copies of *EMICERI* in A375 cells. To construct the pAS HDR plasmids, for each sgRNA the HDR templates, which consisted of the 850–900-bp genomic regions flanking the sgRNA cleave site, were PCR amplified from A375 cell genomic DNA using KAPA HiFi HotStart Readymix (KAPA Biosystems KK2602). Then three pAS sequences in tandem (in the order listed above) flanked by the HDR templates were cloned into pUC19 (Addgene 50005). To insert pAS downstream of the *EMICERI* TSS, three rounds of HDR were performed with a different sgRNA and respective pAS HDR plasmid at each round, such that selected clones contained pAS sequences in one copy of *EMICERI* in the first round, two copies in the second round, and three copies in the third round. At each round of HDR, A375 cells were nucleofected with 4 µg sgRNA and Cas9 plasmid (Addgene 52961) and 2.5 µg pAS HDR plasmid using SF Cell Line 4D-Nucleofector X Kit L (Lonza V4XC-2024) according to the manufacturer's instructions. Cells were then seeded sparsely ( $5 \times 10^4$  cells per 10-cm Petri dish) to form single-cell clones. After 24 h, cells were selected for Cas9 expression with 1 µg/ml puromycin for 2 days and expanded until colonies could be picked (~5 days).

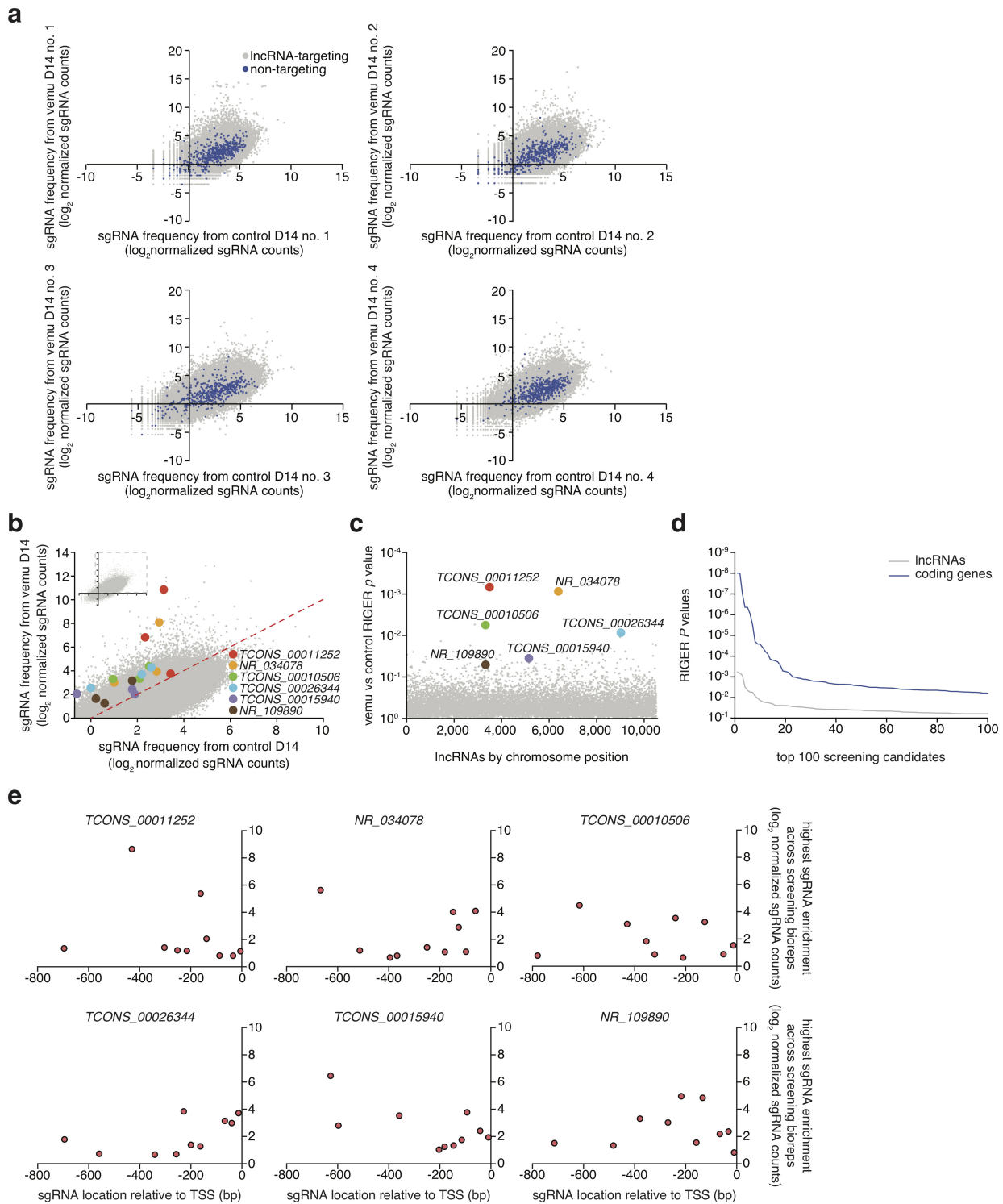
To pick colonies, cells were detached by replacing the medium with PBS and incubating at room temperature for 15 min. Each cell colony was removed from the Petri dish using a 200-µl pipette tip and transferred to a well in a 96-well plate for expansion. Clones with pAS insertions were identified by 2-round PCR amplification (Supplementary Table 9), first with primers amplifying outside the HDR template (HDR primer F1 and HDR primer R, 20 cycles) and then with primers amplifying the region of insertion (HDR primer F2 and HDR primer R, 15 cycles) to avoid detecting the HDR template plasmid as a false positive. Products were run on a 2% agarose gel to identify insertions and Sanger sequencing confirmed that the pAS sequences had been inserted at the appropriate sites. During each round of HDR, three clones with pAS insertions and one clone without pAS insertion (wild type) were selected for further expansion and characterization. The wild-type clone controls for potential on- and off-target indels.

**ASO knockdown.** ASOs targeting *EMICERI*, *EMICERII* and *MOB3B* were custom-designed using Exiqon's Antisense LNA GapmeR designer (Supplementary Table 10) and a non-targeting ASO (Exiqon 300610) was included for control. ASOs were resuspended in water to a final concentration of 100 µM. A375 cells stably expressing SAM components dCas9-VP64 and MS2-p65-HSF1 were nucleofected with 500 ng sgRNA (Supplementary Table 7; Addgene 73795) and 100 pmol ASO using the SF Cell Line 4D-Nucleofector X Kit S (Lonza V4XC-2032) according to the manufacturer's instructions. Cells were then seeded at  $3 \times 10^4$  cells per well in a 96-well plate with four biological replicates per condition. Twenty-four hours after nucleofection, cells were selected for the sgRNA plasmid with 1 µg/ml puromycin (Thermo Fisher A1113803) for 2 days and changes in transcript expression were determined by qPCR as described above.

**Code availability.** Code for lncRNA library design and the analyses described in this paper is available on Github ([https://github.com/fengzhanglab/LncRNA\\_Screen\\_Manuscript](https://github.com/fengzhanglab/LncRNA_Screen_Manuscript)). Please note that the code is published as is for reference.

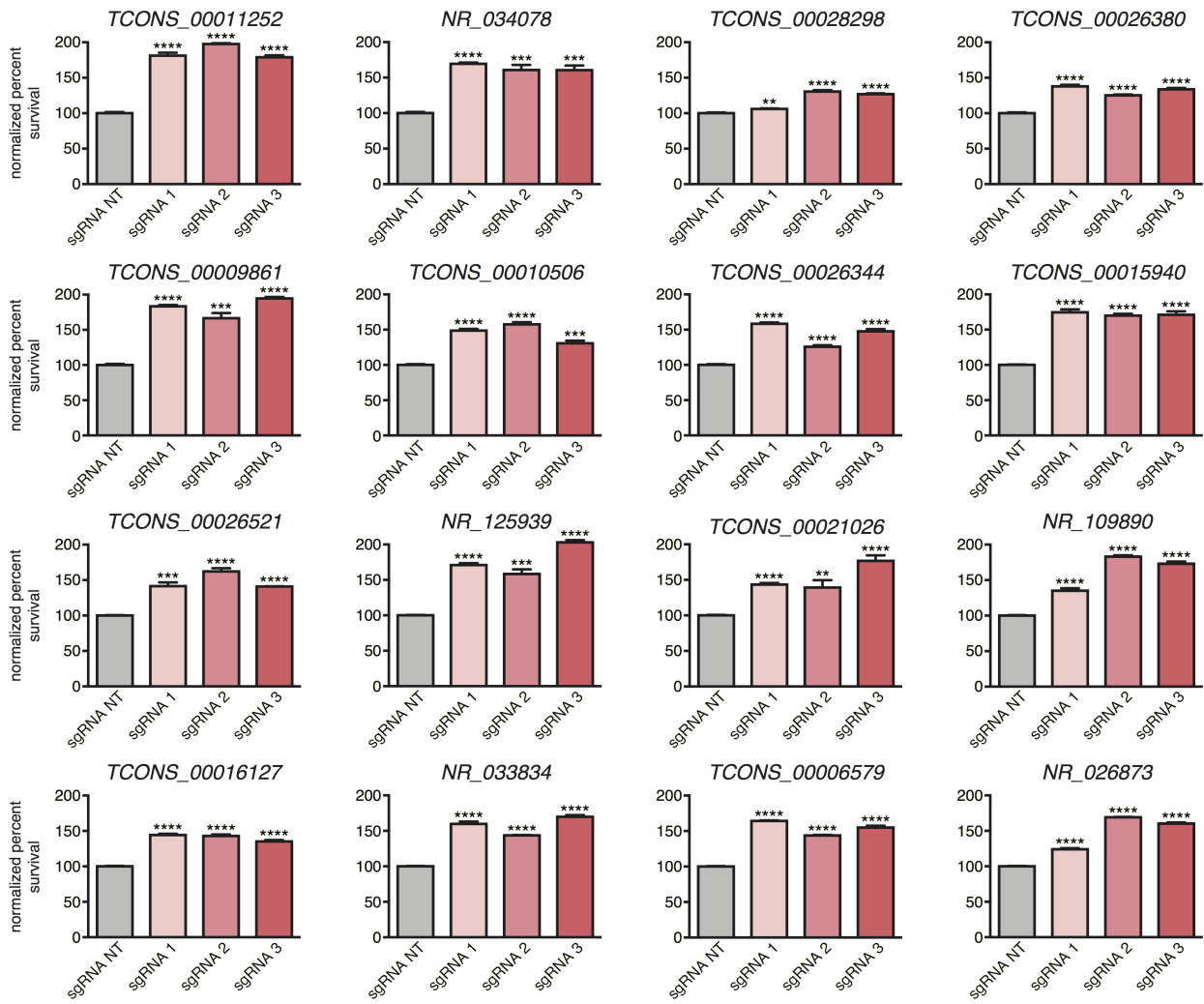
**Data availability.** Sequencing data for this study are available through the Gene Expression Omnibus (GSE99836) and Bioproject (PRJNA324504). All additional data are available from the authors upon reasonable request. The lncRNA library and associated SAM plasmids are available from Addgene under UBMTA.

- Joung, J. *et al.* Genome-scale CRISPR–Cas9 knockout and transcriptional activation screening. *Nat. Protocols* **12**, 828–863 (2017).
- Langmead, B., Trapnell, C., Pop, M. & Salzberg, S. L. Ultrafast and memory-efficient alignment of short DNA sequences to the human genome. *Genome Biol.* **10**, R25 (2009).
- Li, B. & Dewey, C. N. RSEM: accurate transcript quantification from RNA-Seq data with or without a reference genome. *BMC Bioinformatics* **12**, 323 (2011).
- Trapnell, C., Pachter, L. & Salzberg, S. L. TopHat: discovering splice junctions with RNA-Seq. *Bioinformatics* **25**, 1105–1111 (2009).
- Rao, S. S. *et al.* A 3D map of the human genome at kilobase resolution reveals principles of chromatin looping. *Cell* **159**, 1665–1680 (2014). 10.1016/j.cell.2014.11.021
- Consortium, E. P.; ENCODE Project Consortium. An integrated encyclopedia of DNA elements in the human genome. *Nature* **489**, 57–74 (2012).
- Felsenstein, J. & Churchill, G. A. A Hidden Markov Model approach to variation among sites in rate of evolution. *Mol. Biol. Evol.* **13**, 93–104 (1996).
- Konieczkowski, D. J. *et al.* A melanoma cell state distinction influences sensitivity to MAPK pathway inhibitors. *Cancer Discov.* **4**, 816–827 (2014).
- Barbie, D. A. *et al.* Systematic RNA interference reveals that oncogenic KRAS-driven cancers require TBK1. *Nature* **462**, 108–112 (2009).
- Barretina, J. *et al.* The Cancer Cell Line Encyclopedia enables predictive modelling of anticancer drug sensitivity. *Nature* **483**, 603–607 (2012).

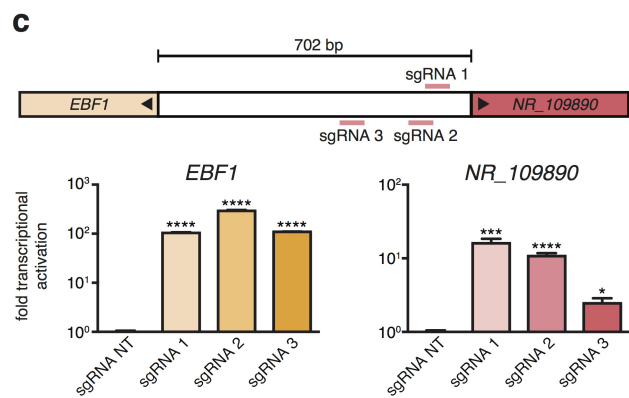
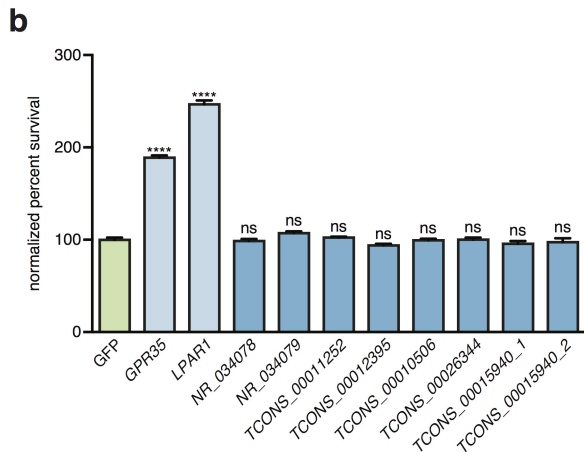
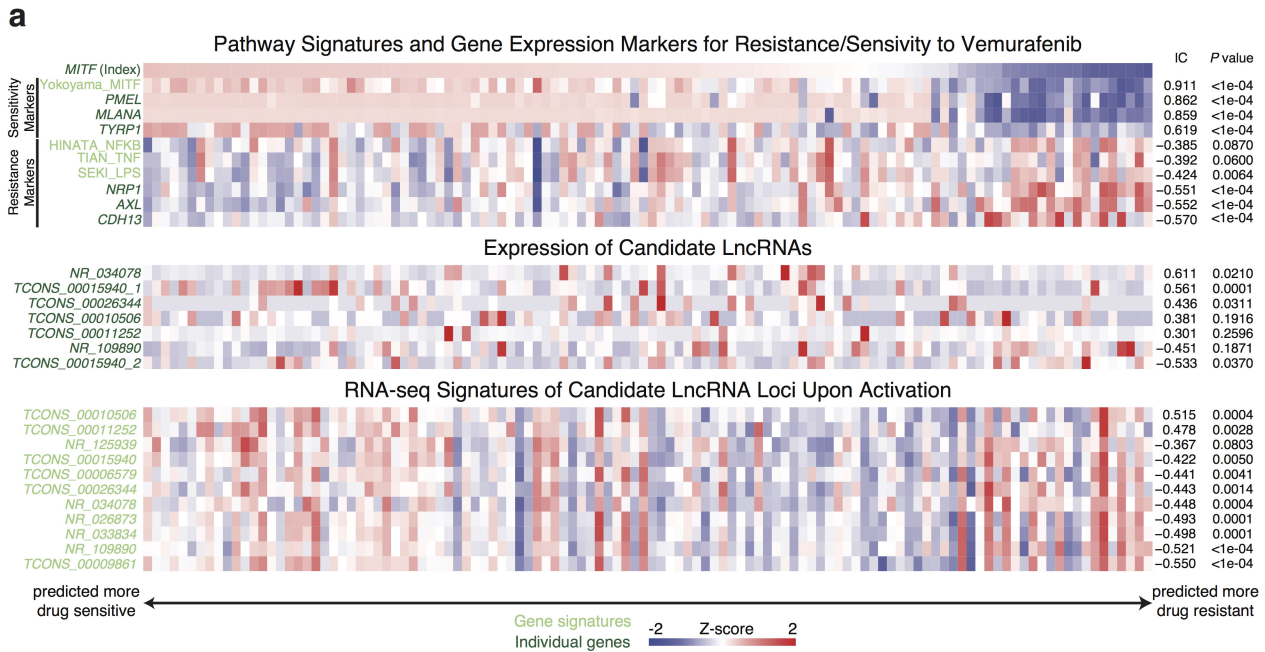


**Extended Data Figure 1 | Genome-scale activation screen for lncRNA loci involved in vemurafenib resistance.** **a**, Scatterplots showing lncRNA-targeting and non-targeting sgRNA frequencies after vemurafenib (vem) or control treatment from  $n = 4$  infection replicates. **b**, Scatterplot showing enrichment of sgRNAs targeting six candidate lncRNA loci. **c**, RIGER  $P$  values of the candidate lncRNA loci. **d**, RIGER  $P$  values for the top 100 hits from the previous SAM protein-coding gene screen<sup>9</sup> compared

to the SAM lncRNA loci screen. **e**, For each candidate lncRNA locus, ten sgRNAs were designed to target the proximal promoter region (800 bp upstream of the TSS). The relationship between the highest sgRNA enrichment in vemurafenib-treated compared to control condition across screening bioreps ( $n = 4$ ) and respective spacer position suggests that sgRNAs targeting closer to the annotated TSS are not necessarily more effective, consistent with previous results<sup>9</sup>.

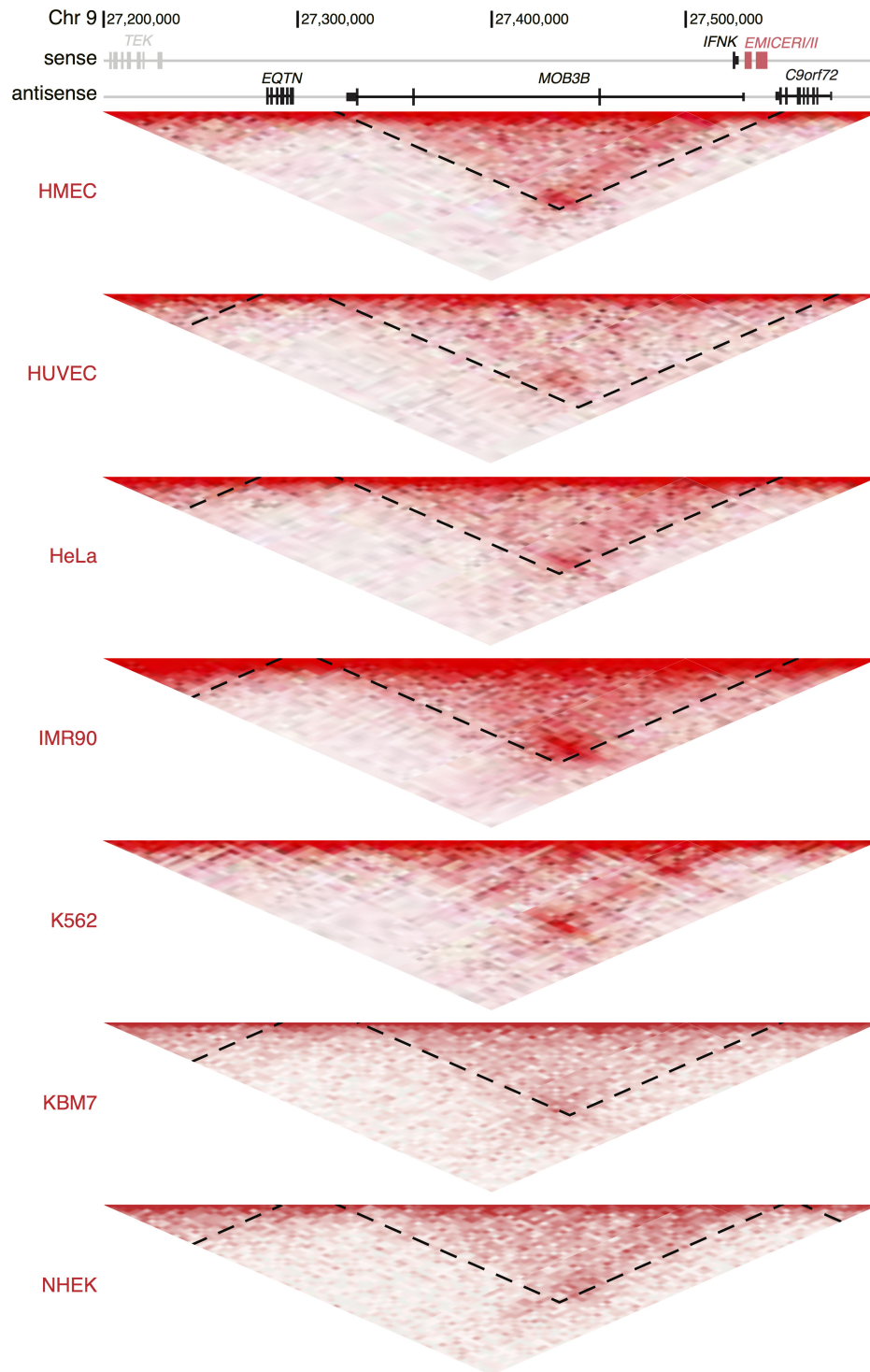


**Extended Data Figure 2 | Validation of candidate lncRNA loci for vemurafenib resistance.** Vemurafenib resistance for A375 cells transduced with SAM and individual sgRNAs targeting the top 16 candidate lncRNA loci normalized to a non-targeting (NT) sgRNA. All values are mean  $\pm$  s.e.m. with  $n = 4$ . \*\*\*\* $P < 0.0001$ ; \*\*\* $P < 0.001$ ; \*\* $P < 0.01$ .



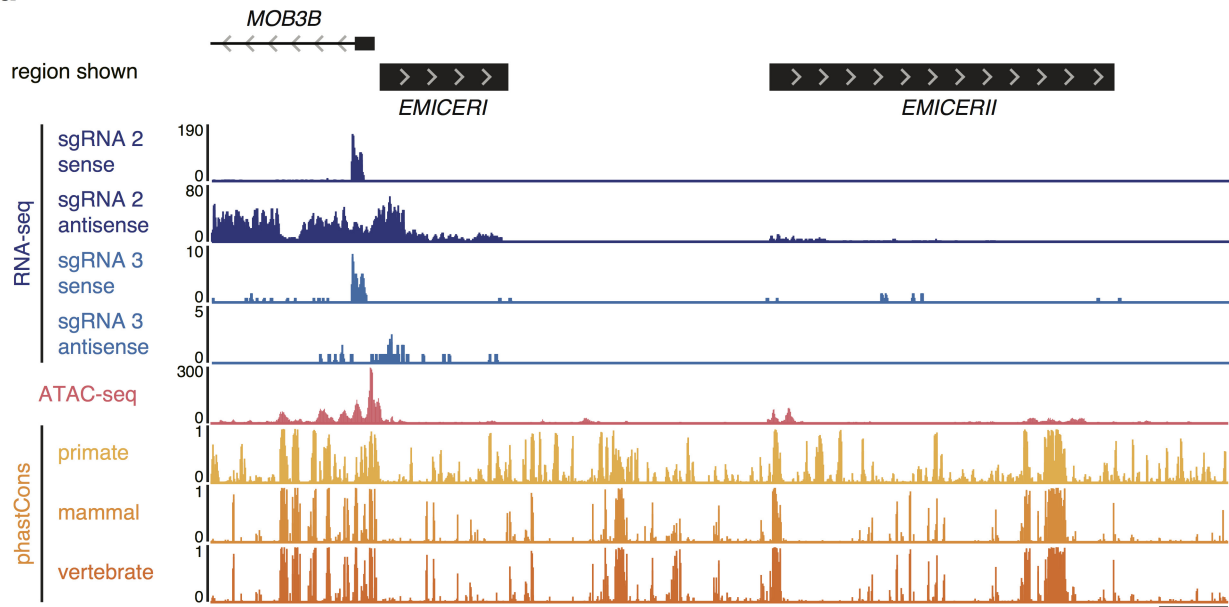
**Extended Data Figure 3 | Activation of candidate lncRNA loci appears to mediate vemurafenib resistance by regulating expression of nearby genes.** **a**, Heat map showing expression of genes and signature markers for BRAF inhibitor sensitivity (top), expression of candidate lncRNA loci (middle), and RNA-seq signature of gene expression changes upon activation of candidate lncRNA loci (bottom) in 113 different BRAF(V600) patient melanoma samples (primary or metastatic) from The Cancer Genome Atlas. All associations are measured using the information coefficient (IC) between the index and each of the features and  $P$  values are determined using a permutation test. Panels

show Z-scores. **b**, Vemurafenib resistance of A375 cells overexpressing cDNAs encoding each candidate lncRNA or protein-coding gene normalized to GFP. *GPR35* and *LPAR1* are positive controls identified previously<sup>9</sup>. The same set of sgRNAs targeted *TCONS\_00012395* and *TCONS\_00011252*; *NR\_034078* and *NR\_034079*; *TCONS\_00015940\_1* and *TCONS\_00015940\_2*. **c**, Expression of *NR\_109890* and its neighbouring gene *EBF1* after SAM activation of *NR\_109890*. All values are mean  $\pm$  s.e.m. with  $n = 4$ . \*\*\*\* $P < 0.0001$ ; \*\*\* $P < 0.001$ ; \* $P < 0.05$ . ns, not significant.

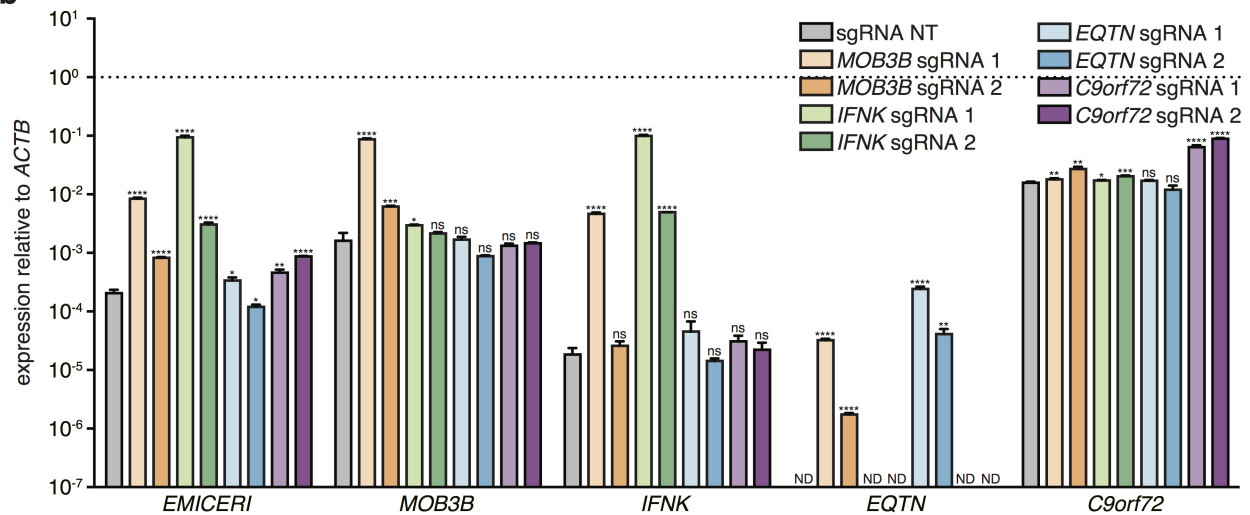


**Extended Data Figure 4 | Topological domain in the *EMICERI* locus is consistent across cell types.** Hi-C data and topological domain annotations (dotted lines) in the *EMICERI* locus from seven cell lines<sup>23</sup>. Heat map shows KR-normalized contact matrix at 5-kb resolution. Domain annotations for chromosome 9 were not available in K562, but the same topological domain structure is evident.

a

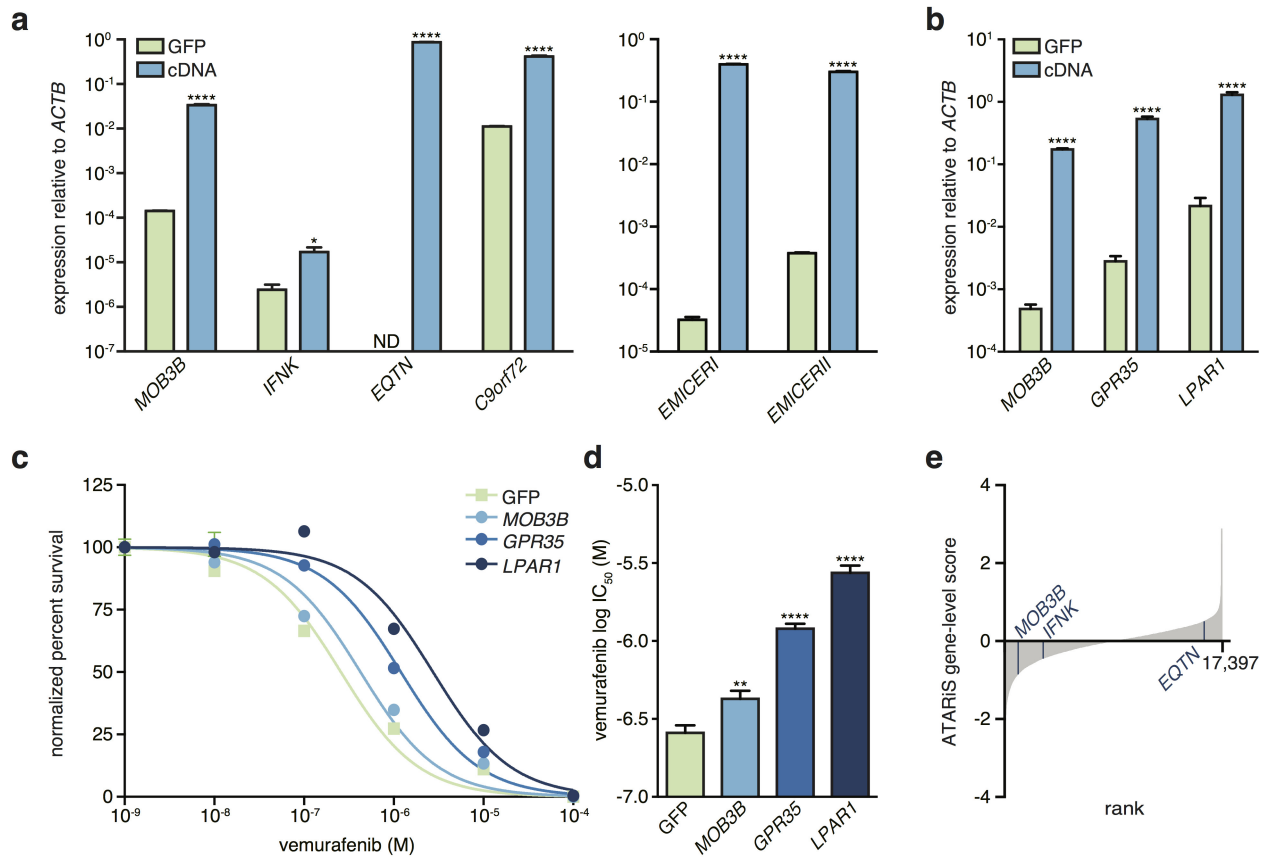


b



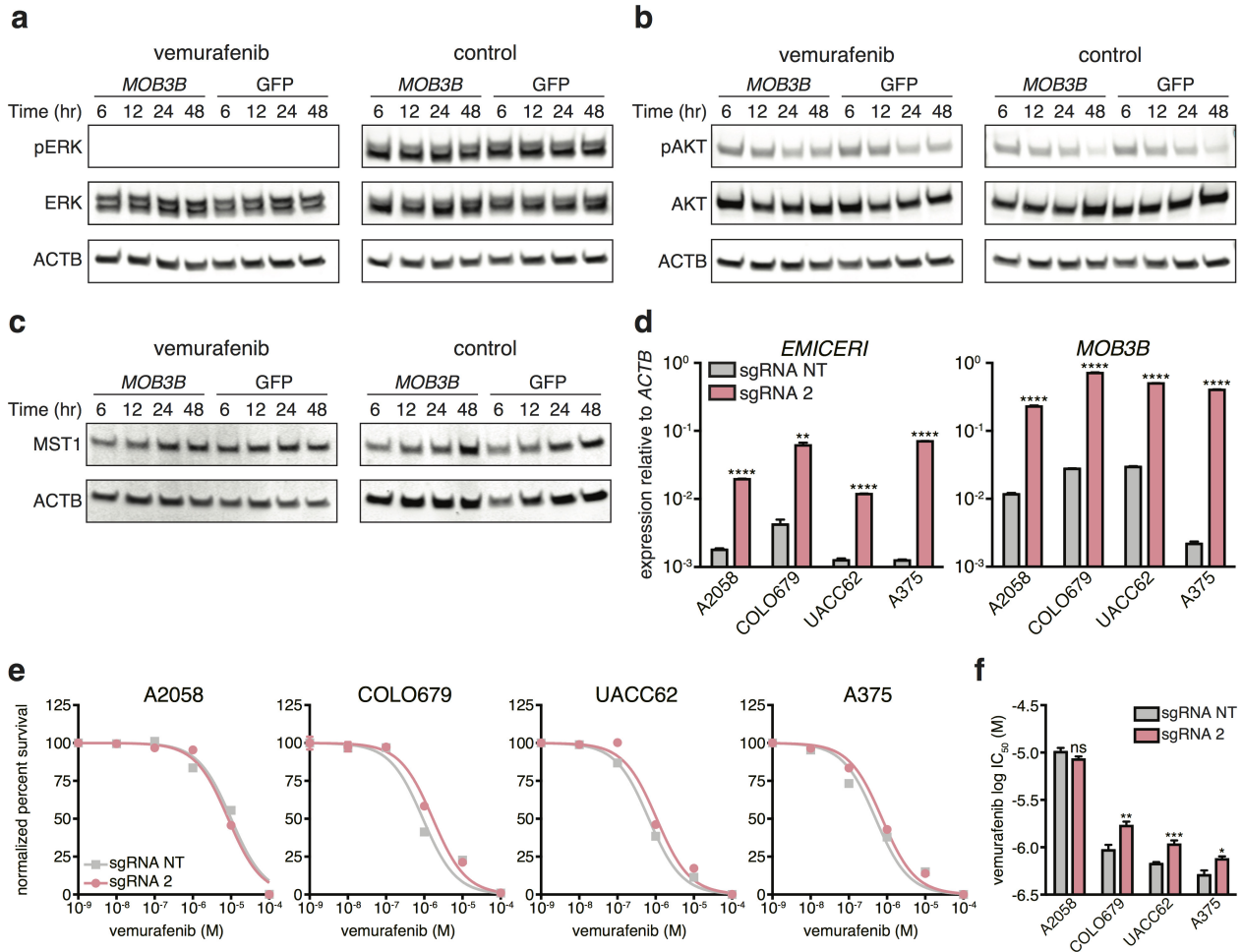
**Extended Data Figure 5 | Dosage-dependent upregulation of the *EMICERI* locus is specific to activation of *EMICERI* at its conserved regulatory element.** a, TopHat alignment of RNA-seq paired-end reads suggests that *EMICERI* is located at chr9:27,529,917–27,531,782 and *EMICERII* at chr9:27,535,71–27,540,711 (UCSC hg19) (Supplementary Note 6). A375 ATAC-seq and phastCons conservation scores for primates,

placental mammals, and vertebrates at the *EMICERI* locus. Scale bar, 1 kb. b, Expression of *EMICERI* and its neighbouring genes *MOB3B*, *IFNK*, *EQTN* and *C9orf72* after transduction with sgRNAs targeting SAM to the promoters of neighbouring genes. All values are mean  $\pm$  s.e.m. with  $n = 4$ . \*\*\*\* $P < 0.0001$ ; \*\*\* $P < 0.001$ ; \*\* $P < 0.01$ ; \* $P < 0.05$ . ns, not significant. ND, not detected.



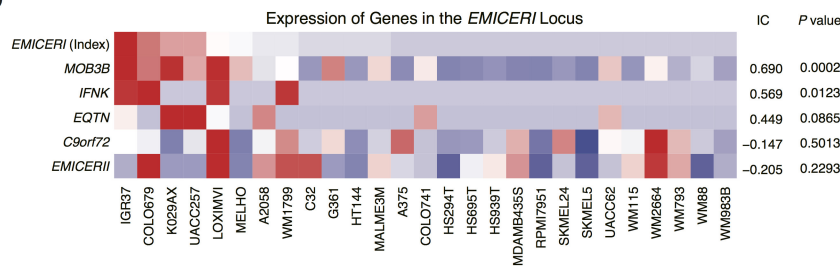
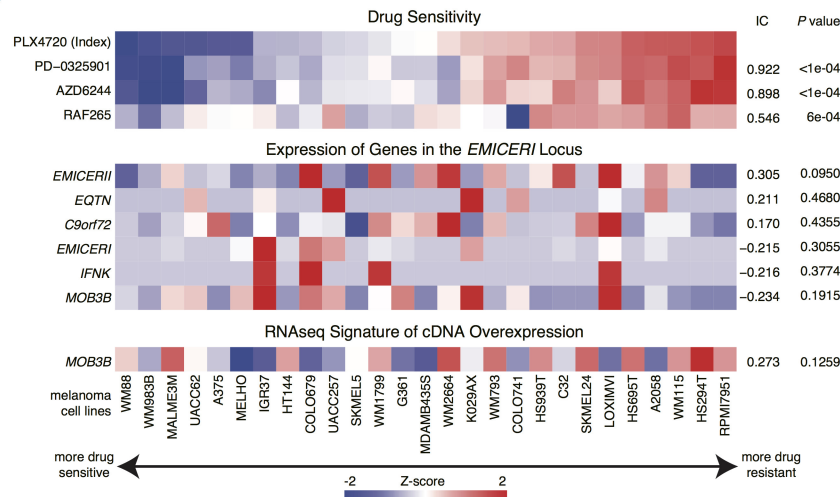
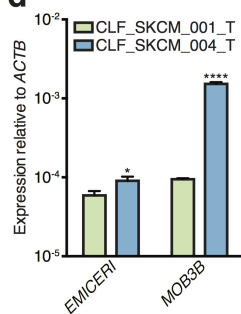
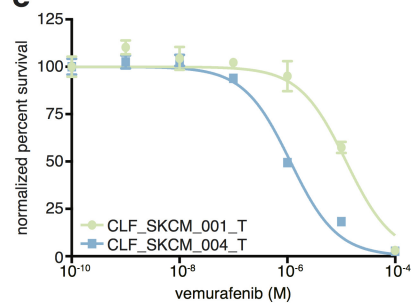
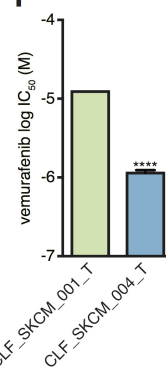
**Extended Data Figure 6 | Activation of *EMICER1* mediates vemurafenib resistance through *MOB3B*.** **a**, Expression of the neighbouring genes or *EMICER1* or *EMICER2* after cDNA overexpression compared to GFP control. **b**, cDNA overexpression of top hits from the SAM protein-coding gene screen for vemurafenib resistance (*GPR35* and *LPAR1*)<sup>9</sup> or *MOB3B* compared to GFP control. **c**, Vemurafenib dose response curves for A375 cells overexpressing cDNA or GFP control. **d**, Vemurafenib half

maximal inhibitory concentration (IC<sub>50</sub>) for the same conditions as in **c**. **e**, ATARIS gene-level scores from the Achilles Project that reflect genetic vulnerabilities of A375 cells. Lower ATARIS gene-level scores indicate stronger dependency on the gene. Rank of *MOB3B*, 1,084; *IFNK*, 3,078; *EQTN*, 15,939. All values are mean ± s.e.m. with *n* = 4. \*\*\*\**P* < 0.0001; \*\**P* < 0.01; \**P* < 0.05. ND, not detected.



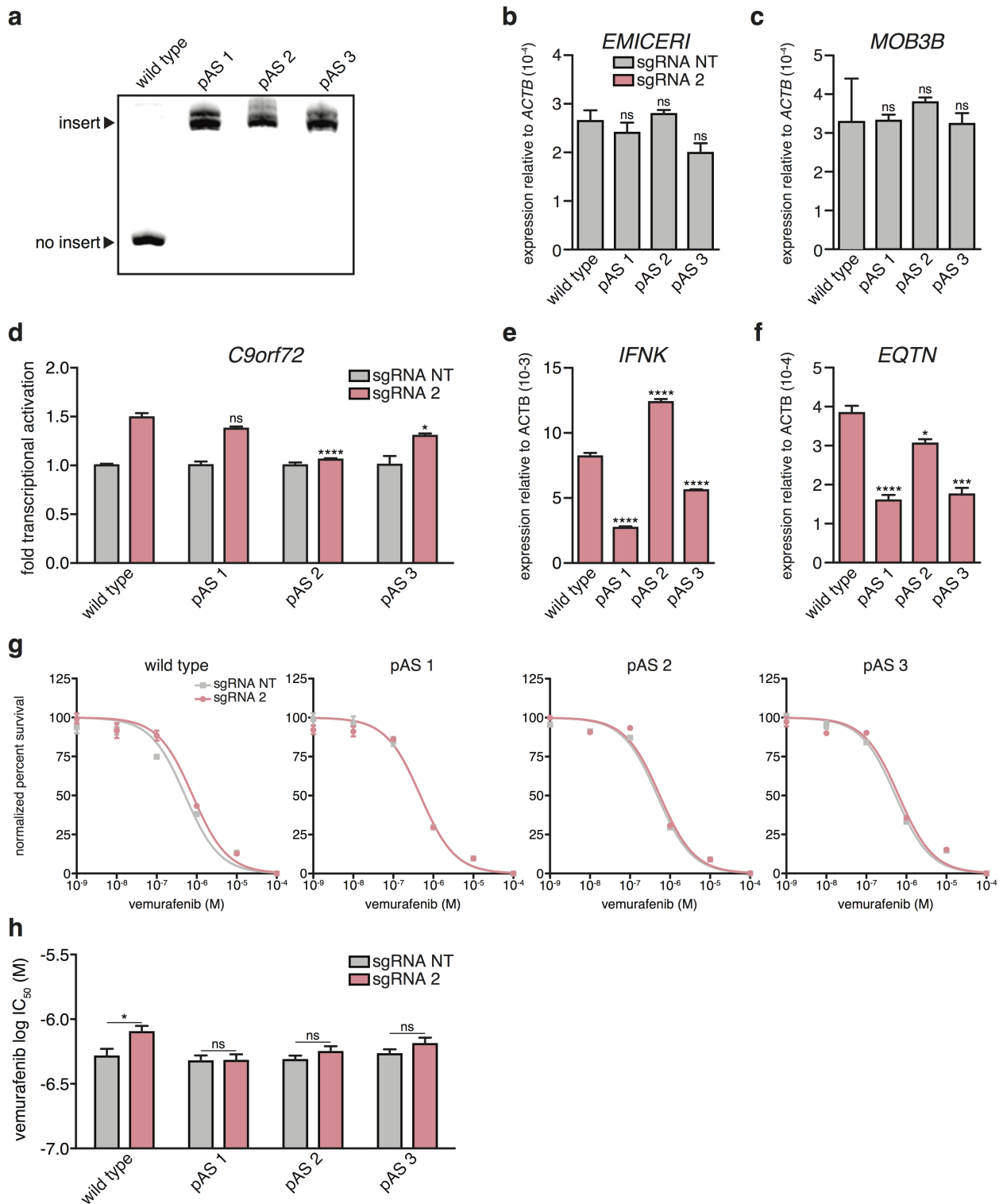
**Extended Data Figure 7 | Activation of *EMICERI* mediates vemurafenib resistance in melanoma cell lines.** **a–c**, Western blots of A375 cells stably overexpressing *MOB3B* cDNA or GFP control after vemurafenib or control (DMSO) treatment. For gel source data, see Supplementary Fig. 1. **d**, Expression of *EMICERI* and *MOB3B* after SAM activation in different

melanoma cell lines. **e**, Vemurafenib dose response curves for *EMICERI* activation in different melanoma cell lines. **f**, Vemurafenib half maximal inhibitory concentration ( $IC_{50}$ ) for the same conditions as in **e**. All values are mean  $\pm$  s.e.m. with  $n = 4$ . \*\*\*\* $P < 0.0001$ ; \*\*\* $P < 0.001$ ; \*\* $P < 0.01$ ; \* $P < 0.05$ . ns, not significant.

**a****b****c****d****e****f**

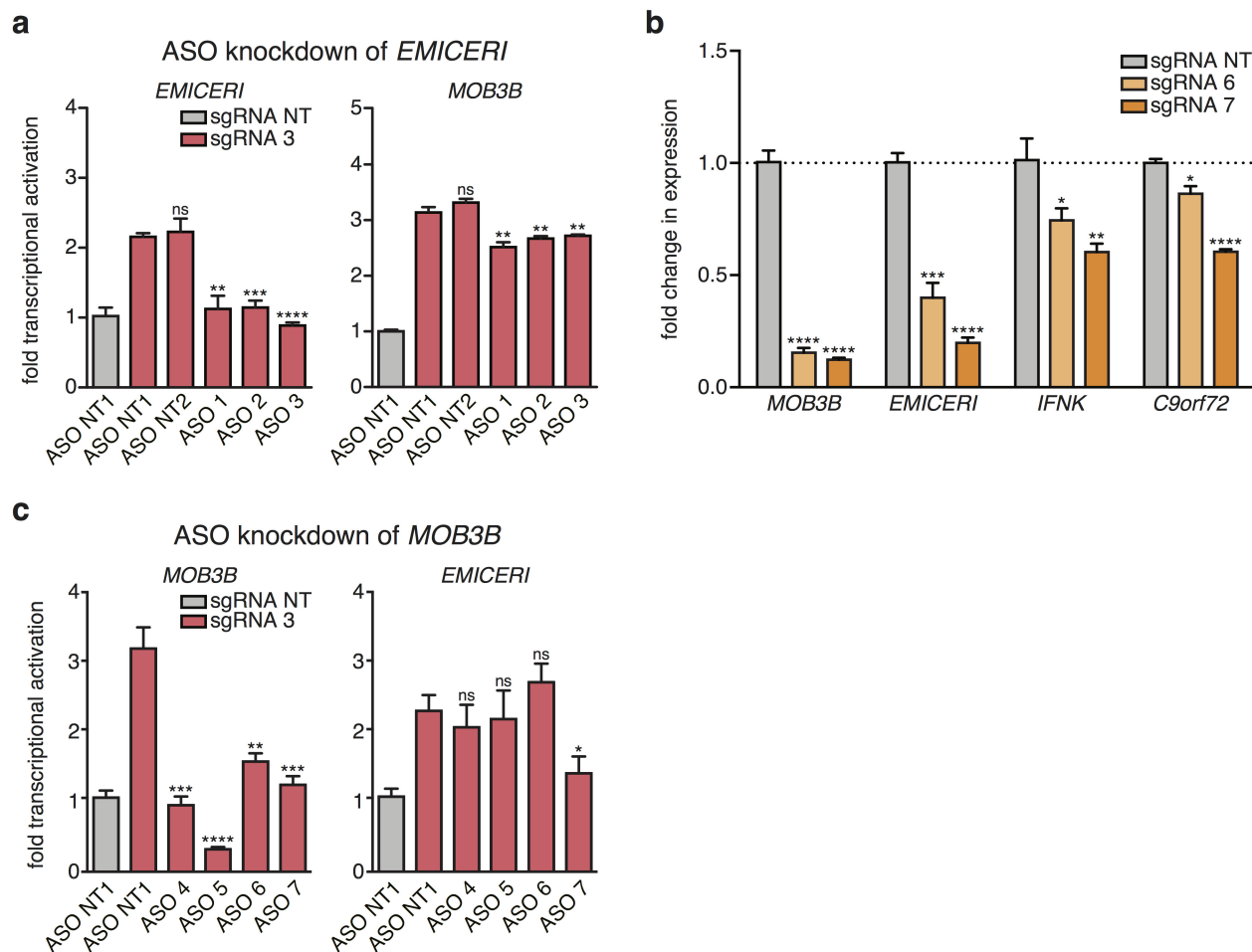
**Extended Data Figure 8 | *EMICERI* expression is strongly correlated with *MOB3B* expression and vemurafenib sensitivity in melanoma cell lines and patient samples.** **a**, Heat map showing expression of genes in the *EMICERI* locus in 113 different BRAF (V600) patient melanoma samples (primary or metastatic) from The Cancer Genome Atlas. Samples are sorted by *EMICERI* expression. **b**, Heat map showing expression of genes in the *EMICERI* locus in melanoma cell lines from the Cancer Cell Line Encyclopedia (CCLE) sorted by *EMICERI* expression. **c**, Heat map showing sensitivity to different drugs (top), expression of genes in the *EMICERI* locus (middle), and *MOB3B* cDNA overexpression RNA-seq signature (bottom; see Methods for signature generation) in melanoma cell lines from CCLE. Drug sensitivities are measured as Activity Areas.

The melanoma cell lines are sorted by PLX-4720 (vemurafenib) drug sensitivity. RAF inhibitors: PLX-4720 and RAF265; MEK inhibitors: AZD6244 and PD-0325901. **d**, Expression of *EMICERI* and *MOB3B* in two primary patient-derived BRAF(V600E) melanoma cell lines. **e**, Vemurafenib dose response curves for the same cell lines. **f**, Vemurafenib half maximal inhibitory concentration ( $IC_{50}$ ) for the same conditions as in **e**. All associations are measured using the information coefficient (IC) between the index and each of the features and  $P$  values are determined using a permutation test. Heat maps show Z-scores. All values are mean  $\pm$  s.e.m. with  $n = 4$ . \*\*\*\* $P < 0.0001$ ; \* $P < 0.05$ .



**Extended Data Figure 9 | Transcriptional activation of *EMICERI* modulates expression of neighbouring genes to confer vemurafenib resistance.** **a**, Gel confirming pAS insertion into all three copies of *EMICERI* for each pAS clone. For gel source data, see Supplementary Fig. 1. **b**, **c**, Basal expression of *EMICERI* and *MOB3B* for the wild-type and pAS clones. **d**–**f**, Expression of *C9orf72*, *IFNK* and *EQTN*

after targeting *SAM* to *EMICERI* for the wild-type and pAS clones. **g**, Vemurafenib dose response curves for wild-type and pAS clones transduced with *SAM* and *EMICERI*-targeting or non-targeting (NT) sgRNAs. **h**, Vemurafenib half-maximal inhibitory concentration ( $IC_{50}$ ) for the same conditions as in **g**. All values are mean  $\pm$  s.e.m. with  $n = 4$ . \*\*\*\* $P < 0.0001$ ; \*\*\* $P < 0.001$ ; \* $P < 0.05$ . ns, not significant.



**Extended Data Figure 10 | Transcriptions of *EMICERI* and *MOB3B* act reciprocally to regulate each other.** **a**, Expression of *EMICERI* and *MOB3B* after ASO knockdown of *EMICERI* in the context of SAM activation. **b**, Expression of *MOB3B* and neighbouring genes in A375 cells transduced with non-targeting (NT) or *MOB3B*-targeting sgRNAs and

dCas9. **c**, Expression of *MOB3B* and *EMICERI* after ASO knockdown of *MOB3B* in the context of SAM activation. All values are mean  $\pm$  s.e.m. with  $n = 4$ . \*\*\*\* $P < 0.0001$ ; \*\*\* $P < 0.001$ ; \*\* $P < 0.01$ ; \* $P < 0.05$ . ns, not significant.